PHILOSOPHICAL TRANSACTIONS OF THE ROYAL SOCIETY A
MATHEMATICAL, PHYSICAL & ENGINEERING SCIENCES

Water entry and exit of horizontal circular cylinders

Martin Greenhow and Simiso Moyo

Phil. Trans. R. Soc. Lond. A 1997 **355**, 551-563
doi: 10.1098/rsta.1997.0024

Water entry and exit of horizontal circular cylinders

By Martin Greenhow and Simiso Moyo
Department of Mathematics and Statistics, Brunel University, Uxbridge, Middlesex UB8 3PH, UK

This paper describes fully nonlinear two-dimensional numerical calculations of the free-surface deformations of initially calm water caused by the forced motion of totally or partially submerged horizontal circular cylinders. The paper considers the following.

(i) Totally submerged cylinders moving with constant velocity in vertical, horizontal or combined motions. Results are compared with the small-time asymptotic solution obtained by Tyvand & Miloh in 1995. Their results, which are taken to third-order (which is when gravity terms first appear in the expansions), are in excellent agreement with the numerical calculations for small times; beyond this only the numerical method gives accurate results until the free surface breaks or the cylinder emerges from the free surface. Breaking can occur during exit due to strongly negative pressures arising on the cylinder surface, or during the downwards motion causing a free-surface depression which closes up rapidly, forming splashes. Downwards motion is also shown to give rise to high-frequency waves in some cases.

(ii) The free-surface deformations, pressures and forces acting on a cylinder in vertical or oblique forced motion during engulfment when it submerges from being initially half-submerged. The initial stages, when the cylinder still pierces the free surface, specify the initial conditions for a separate program for a completely submerged body, thereby allowing complete engulfment to be studied. The free surface closes up violently over the top of the cylinder resulting in jet flow, which, while difficult to handle numerically, has been shown to be insignificant for the bulk flow and the cylinder pressures and forces.

1. Introduction

The two-dimensional interaction of solid bodies with the free surface is of major importance in many engineering contexts, especially in ocean and coastal engineering, since it usually represents worst-case design loading. Examples in these fields include wave loading in the splash zone on oil rigs, marine operations where units are lowered from a crane ship through the free surface, earthquake and other extreme loading on floating bridges and dams, interaction of waves with pipelines, impact of sloshing fluid on baffles in tanks, impact of steep waves on breakwaters and other fixed structures such as wave energy devices, ship slamming and extreme ship motions. The physical and mathematical modelling of the situations is complex, involving body elasticity, air and air/water mixture compressibility effects, at least in the early stages of impact, and viscous effects causing vortex shedding in the later

Phil. Trans. R. Soc. Lond. A (1997) **355**, 551–563
Printed in Great Britain

stages. The experimentalist faces difficult problems of sensitivity to initial conditions and repeatability for the early stages, and scaling for all stages of the fluid-structure interaction. In particular, the energy in the fluid, expressed in terms of the added mass, is strongly dependent on the cylinder's proximity to the fluid boundary, see Bassett (1888) and Greenhow & Li (1987), and this gives rise to inviscid forces which are proportional to the body velocity squared; this makes it difficult, or impossible, to separate viscous loading (also proportional to v^2 according to Morison's equation) which requires Reynold's scaling, from the inviscid loading, which requires Froude scaling.

It is therefore necessary to simplify the problem before attempting any analytical or numerical solution. We here consider only the inviscid loading, due to two-dimensional fluid motion in the vertical plane, on horizontal circular cylinders moving in initially calm deep water, but we do not make any further linearising assumptions on the free-surface or body boundary conditions. In particular, we study the exit of the body as well as the entry phase. In some ways the exit phase is less amenable to theoretical treatment (gravity cannot be ignored for example), but is nevertheless important since it can give rise to appreciable hydrodynamic forces which may affect the body motion and therefore the subsequent slamming forces and pressures upon re-entry in the case of ship slamming in extreme ship motions; see Barringer (1996).

The submerged circular cylinder/free surface interaction problem has a long history dating at least from Havelock's work (1936, 1949*a*,*b*) on impulsively started constant velocity or accelerated horizontal motion. The time-dependent free surface is linearized and the cylinder represented as a dipole moving beneath it, giving rise to an image dipole above the free surface and an explicit memory integral over the previous cylinder motion arising from previously generated radiated waves. This memory term in the velocity potential gives rise to steady forces and transient oscillatory forces on the body, both of which are only qualitatively correct when compared with fully nonlinear calculations of the type considered here, see Haussling & Coleman (1979), Hepworth (1991) and Greenhow (1993). The large-time asymptotic form of the oscillatory forces are corrected by Lui & Yue (1996), giving results which are in close agreement with their direct numerical calculations. For vertically moving cylinders, Sakai *et al.* (1933) considered a vertically moving dipole as a model, but when it is near the free surface the large free-surface deformations make the assumed linearized boundary conditions there invalid. Tuck (1965) considered the horizontal motion steady state problem correct to second order in wave steepness, while Tyvand & Miloh (1995*a*, *b*) considered the dipole moved impulsively in any direction under a fully nonlinear free surface.

An alternative approach is to consider the linearized frequency-domain model usually used in ship hydrodynamics. Early papers by Dean (1948), Ursell (1950), Ogilvie (1963), Evans *et al.* (1979) and others, solved the steady-state sinusoidal problems of waves diffracting over a fixed body, or that of a moving body radiating waves in otherwise calm water. The diffraction and radiation problems have been solved to second order in wave steepness by, for example, Ogilvie (1963) and Wu (1993), respectively.

The above approaches are useful when considering the loads on a marine structure under normal working conditions, but fail to give accurate results for the extreme situations considered here. What is needed is a method which accounts correctly for both the nonlinearity of the free-surface boundary conditions, and the fact that the body condition, while appearing to be linear, must be applied not on the 'mean' position of the body surface, but on its actual position (which for free motion will not be known *a priori*). This second requirement means that series expansion methods which apply boundary conditions on the initial body surface position are only valid for small times after the motion has started. The impulsively started constant velocity or constantly accelerated motion of a vertical wavemaker has been studied using such series expansions by Peregrine (unpublished note) and King & Needham (1994), whilst the corresponding problems for a submerged circular cylinder have been solved to third-order by Tyvand & Miloh (1995a, b), see below.

These solutions form the basis for accurate comparisons with free-surface profiles calculated by the numerical method for submerged or surface-piercing bodies given below, based on the work of Vinje & Brevig (1981a,b), followed by Brevig *et al.* (1981), Telste (1987), Greenhow (1987), Terent'ev (1991), Hepworth (1991) and Greenhow (1993). Although no direct comparison with experiments has yet been attempted, the results of both numerical and analytical methods are qualitatively very similar to the photographs taken by Greenhow & Lin (1983) for both the horizontal motion of the wavemaker, and the vertical motion of cylinders (up and down) and wedges (downwards only). For such wedge entry at high Froude number (neglecting gravity), the flow is known to be self-similar, see Wagner (1932), and Howison *et al.* (1991) for a modern treatment. Self-similarity implies that the arc length between free-surface Lagrangian marker particles is conserved, (Garabedian 1953; Fraenkel, this volume); this provides a stringent check on the accuracy of the present numerical method (Greenhow 1987). It was found that the numerical method for surface-piercing bodies of Vinje & Brevig (1981a) gives accurate results if the initial deadrise angle (between the fluid and body surfaces at their intersection) is not smaller than about 45°, and we do not violate this restriction in the present calculations. For smaller deadrise angles, Zhao & Faltinsen (1993) have given accurate results for the body forces and pressures, but they cut off the ejected spray jets in their numerical scheme. This procedure is sensible since the jets are thin and have almost atmospheric pressure throughout; we adopt a similar procedure here to remove jets which would otherwise cause numerical breakdown.

2. Numerical Methods

The numerical methods used are based on the work of Longuet-Higgins & Cokelet (1976) and Vinje & Brevig (1981a,b). Those authors point out that since the irrotational, incompressible flow is two-dimensional, it may be described by either the velocity potential ϕ or a stream function ψ, or, most fundamentally, by a complex velocity potential $\beta = \phi + \mathrm{i}\psi$ which is then analytic in the fluid region. This means that Cauchy's theorem holds for any contour lying within, or at the boundary of, the fluid. Choosing a contour C around the boundary therefore results in

$$\oint_C \frac{\beta(z)}{z - z_0}\mathrm{d}z = 0, \tag{2.1}$$

where z_0 lies outside C. Now C may be split into two parts: C_ϕ where ϕ is known and C_ψ where ψ is known, see figure 1; these quantities are either specified initially or known from the evolution equations below. Thus ϕ and its time derivative are known on the free surface ($D\phi/Dt$ is given from the Bernoulli equation), while ψ and its time derivative are known on the bottom (both vanish here) and on a body surface (ψ and $\partial\psi/\partial t$ are here specified by the body geometry and its velocity or

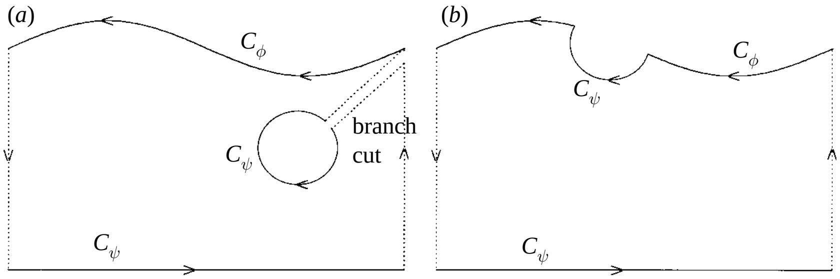

Figure 1. Contours of integration for the submerged (*a*) and surface-piercing (*b*) body cases.

acceleration, respectively). Letting $z_0(=x_0+\mathrm{i}y_0)$ approach the contour C, and using either the real or imaginary parts of equation (2.1), gives integral equations of the second kind:

$$\pi\psi(x_0,y_0,t)+\mathrm{Re}\left[\int_C \frac{\phi+\mathrm{i}\psi}{z-z_0}\mathrm{d}z\right]=0 \tag{2.2}$$

for z_0 on C_ϕ, and

$$\pi\phi(x_0,y_0,t)+\mathrm{Re}\left[\mathrm{i}\int \frac{\phi+\mathrm{i}\psi}{z-z_0}\mathrm{d}z\right]=0 \tag{2.3}$$

for z_0 on C_ψ. Similar equations hold for the time derivative of β. We have further assumed that C is smooth; at corners, either due to the presence of a solid body or due to discretization of C, we use the angle θ subtended by the collocation points in place of π in these equations. On the vertical boundaries in figure 1, we apply periodicity for convenience, but the precise condition here is not relevant for the present short time calculations since they are placed so far away from the body that no noticeable waves ever reach them during the time of the calculations.

To step forward in time we use the boundary conditions for the two-dimensional free-surface problem. Following Longuet-Higgins & Cokelet (1976), we write the free surface conditions following a free-surface particle (a Lagrangian description of the flow) as

$$\frac{Dz}{Dt}=u+\mathrm{i}v=w^*=\frac{\partial\beta}{\partial z}, \tag{2.4}$$

$$\frac{D\Phi}{Dt}=ww^*-gy-\frac{P_s}{\rho}, \tag{2.5}$$

where g is the gravity, ρ is the density, * denotes complex conjugate, and the material derivative is given by

$$\frac{D(\,)}{Dt}=\frac{\partial(\,)}{\partial t}+\nabla\phi\cdot\nabla(\,). \tag{2.6}$$

These equations are used to evolve the position and value of ϕ of the free-surface particles to the next time step. Specifically a single step Runge–Kutta method is used to calculate the first three steps, after which we may use a fourth-order Hamming predictor/corrector method. A numerical spatial derivative of β is calculated. The forces on the body are calculated by integrating the hydrodynamic pressure, given by Bernoulli's equation, over its surface. For further details see Vinje & Brevig (1981), and Brevig *et al.* (1981).

The integral equations for the unknown part of β are solved in the physical plane by using the collocation method and the integrals are evaluated assuming a linear

PHILOSOPHICAL TRANSACTIONS OF THE ROYAL SOCIETY A MATHEMATICAL, PHYSICAL & ENGINEERING SCIENCES

variation between the collocation points. This results in an $N * N$ matrix equation $AX = B$ for the unknown part X of β at each of the N collocation points. The elements of the $N * N$ matrix A consist of logarithmic terms, requiring typically 40% of the calculation time for their evaluation. However, the matrix is also used at each time step for the calculation of the unknown part of $D\beta/Dt$, and could also be used for the calculation of higher derivatives of β, as in the Dold & Peregrine (1986) method. For surface-piercing bodies this is unlikely to be an advantage since the number of collocation points, and hence equations, changes continuously as the body becomes more or less submerged. This also means that iterative schemes for solving the matrix equation are difficult to program, and we use direct Gaussian elimination at each time-step. Another possible refinement used by other authors is to map C in the fluid domain to a closed contour in a mapped plane, thereby avoiding the need to place collocation points down the vertical boundaries (which must be periodic); this does not seem feasible for the general contour geometries needed here.

For surface-piercing bodies a problem occurs at the intersections of the free and body surfaces. Except in special cases, the complex velocity potential β or its time derivatives are known to be singular here (see Roberts 1987; Vinje 1989). The introduction of viscosity may, in principle, be needed. In the present formulation, we have both ϕ and ψ specified at these points. Although no theoretical justification exists, we remove the two intersection points from the calculations and solve an $(N-2)*(N-2)$ system of equations. Then, treating the intersection points as ordinary free-surface points for the purposes of time-stepping appears to give acceptable results, see Lin *et al.* (1984) for the wavemaker problem and Greenhow (1987, 1988) for wedge and cylinder entry.

For submerged bodies, we do not, of course, have the above intersection point problems. However, a difficulty does arise with the integration around the contour, which now involves a branch cut. We account for this when integrating around inner and outer contours in figure 1. Furthermore, for a fixed body, we do not know the value of ψ on its surface, but it is constant at each time-step. Therefore integrating around the cylinder gives

$$\int_{\text{cyl}} \frac{\mathrm{i}\psi}{z - z_0}\mathrm{d}z = \mathrm{i}\psi \int_{\text{cyl}} \frac{\mathrm{d}z}{z - z_0} = 0, \tag{2.7}$$

when z_0 is outside the cylinder, and

$$\mathrm{Re}\left[\mathrm{i}\int_{\text{cyl}} \frac{\mathrm{i}\psi}{z - z_0}\mathrm{d}z\right] = \mathrm{Re}[\mathrm{i}\pi\psi] = 0, \tag{2.8}$$

when z_0 is on the cylinder. Thus the unknown constant value of ψ is immaterial, but may be calculated around the cylinder from equation (2.2) as a check. For the moving cylinders considered here, we do know the variation of ψ around the cylinder from the body boundary condition to within this unknown constant value (see Brevig *et al.* (1981) for details).

3. Free-surface deformations caused by totally submerged cylinders

A major objective of the present work is to compare results from the fully nonlinear numerical scheme applied to an impulsively started constant velocity submerged horizontal circular cylinder of radius a, with those from the small-time expansion method of Tyvand & Miloh (1995*a*, *b*). The reader is referred to that paper for full details, but it is necessary here to outline some of the main results and terminology. The expansion variable $T = Ut/d$, where U is the cylinder speed, t is (real) time and d is the initial cylinder centre depth, is assumed small, whereas the parameters $\varepsilon = a/d$ and $F_r = v/\sqrt{ag}$, which represents a dimensionless Froude number, are not constrained.

The boundary-value problem is solved subject to the cylinder starting with impulsive velocity at $t = 0$. This gives rise to a velocity potential which is assumed to be of the form

$$\phi = H(t)[\phi_0 + t\phi_1 + t^2\phi_2 + t^3\phi_3 + \ldots], \quad -\infty < t < \infty, \tag{3.1}$$

which gives rise to the free-surface elevation

$$\eta = H(t)[\eta_0 + t\eta_1 + t^2\eta_2 + t^3\eta_3 + \ldots], \quad -\infty < t < \infty, \tag{3.2}$$

where we note that the free surface is explicitly a single-valued function of the horizontal coordinate x, so that overturning is prohibited. The functions η_n where $n = 0, 1, 2, 3, \ldots$ are given by closed-form, but rather complicated expressions: $\eta_0 = 0$ since the free-surface is initially flat, η_1 represents a displacement arising from the impulsive velocity potential Φ_0, whilst η_2 arises from two sources of nonlinearity, namely nonlinear terms in the free-surface condition and a geometric nonlinearity arising from the need to apply the body boundary condition on the displaced body surface. Finally η_3 gives the leading-order effect due to gravity which arises from the second-order velocity potential ϕ_2 being inserted into the expanded free-surface condition.

In an effort to specify the domain of applicability of Tyvand & Miloh's solution, we have conducted extensive comparisons with the numerical method for various cylinder velocities. In particular we wanted to answer the question of how small the dimensionless time variable has to be in order for the expansions to give accurate, or even meaningful results, since it would be extremely difficult to extend the expansion to higher orders. Detailed comparisons of the free-surface deformations for various F_r, initial submergence depths and cylinder radii are shown in figures 2 and 3. Further diagrams may be found in Moyo (1997) for $\varepsilon = 0.2, 0.4, 0.8$ and 0.95, and $F_r = 0.2, 0.39$ and 0.78 in vertical, oblique and horizontal motions; we use all this data to draw general conclusions below. (The actual values of the parameters are determined by full-scale design specifications, but may be considered to be arbitrary here.)

Figure 2 shows the free-surface deformations caused by a large cylinder moving vertically upwards in close proximity to the free surface. Even in this rather extreme test, the expansion method gives excellent agreement up to about $T = 0.4$ and then rapidly deteriorates, becoming topologically impossible for the upwards vertical motion case at $T = 0.6$ when the predicted free surface moves inside the cylinder. The numerical scheme, on the other hand, shows no such behaviour, and the motion may be followed for considerably longer, until $T = 1.0$ when the free surface spontaneously breaks due to rapidly increasing negative pressure building up on the cylinder surface which is just under the thin free surface layer covering the cylinder top. (When it becomes thin, this layer of fluid effectively moves with the cylinder, and its topmost point stagnates in that frame of reference. Presumably surface tension effects then become important in uncovering the top of the cylinder so that it can emerge from the fluid, but we have not included them here.) This negative pressure effect was also calculated by Greenhow (1988), and is thought to give

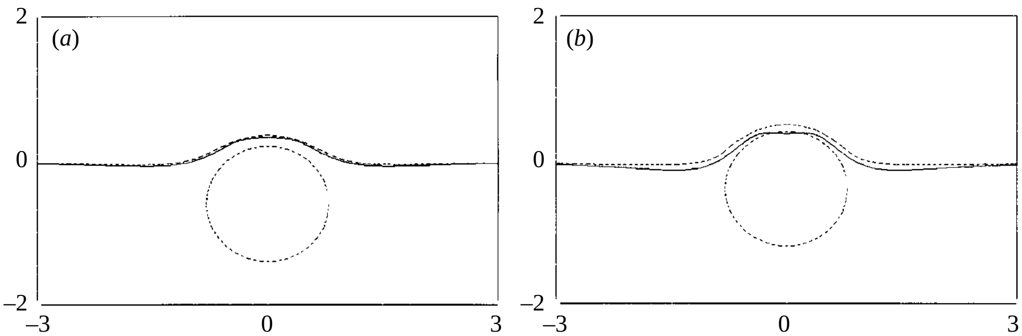

Figure 2. Free-surface disturbance due to a cylinder impulsively started with constant upwards velocity in initially calm water, for dimensionless times ($T = Ut/d$); (a) $T = 0.4$ and (b) $T = 0.6$. The dimensionless parameters are cylinder radius = 0.8 and Froude number = 0.39. The series expansion results of Tyvand & Miloh are shown as solid lines, numerical results are shown dashed.

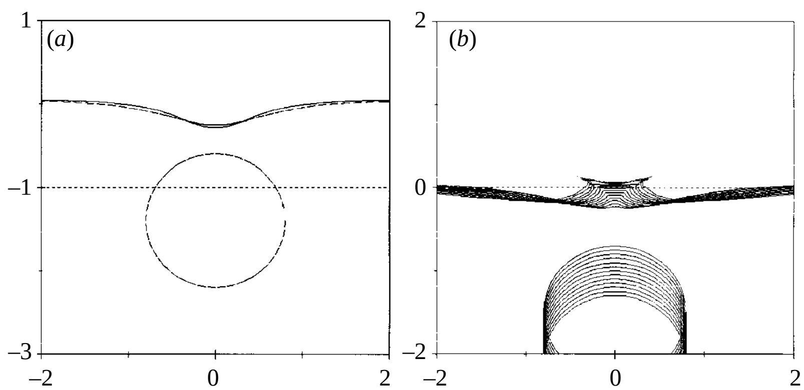

Figure 3. As for figure 2, but with downwards motion, for (a) $T = 0.4$ and (b) $T = 1.0411 \ldots 1.5264$ in steps of 0.0347 (numerical results only).

rise to a type of Rayleigh–Taylor instability and to the rapid violent breaking seen in the photographs of Greenhow & Lin (1983). Despite repeated attempts with other spatial and temporal discretizations, no way could be found to continue the computations and we therefore conclude that such a breakdown is physical rather than numerical. A new feature of Moyo's (1997) calculations is that the same effect also takes place on the trailing side of the obliquely moving cylinder moving upwards at 45°. Such an effect therefore limits, in principle, the ability of purely potential theory to follow the exit beyond the time of breaking. The situation for horizontal motion is different, however; here the pressure within the water remains positive, and the calculations can either be continued indefinitely, or, for larger cylinder velocities, until a well developed breaking wave arises behind the cylinder (see Hepworth 1991; Greenhow 1993).

We are now able to specify approximately the time domain of applicability of the expansion method. It seems quite insensitive to the value of ε (here chosen up to a value of 0.95) and to the direction of cylinder motion, but increases with increasing F_r. Thus for excellent or good agreement between the free surface profiles with $F_r = 0.39$ one must have $T < 0.4$, whilst for $F_r = 0.78$ one must have $T < 0.6$. Beyond these times the comparison becomes inaccurate and then meaningless.

The second major objective of this paper is to consider the free surface motions caused by a cylinder as it moves downwards through the free surface and this is explored in the next section. It is, however, useful to explore the downward motion of an already submerged cylinder, in order to highlight any numerical problems that might arise in the more complicated problem of cylinder engulfment. Comparison with the Tyvand & Miloh expansion method is possible in this case also, see figure 3. Again we are here largely concerned with the free surface deformations since the pressures and forces are dominated by hydrostatics, except when the depression caused by the sinking cylinder rapidly fills and results in a sort of overdriven standing wave which breaks symmetrically outwards, see figure 3. This is caused by an increase of pressure below that portion of free surface, and we see precisely that effect on the top of the cylinder (see Moyo (1997) for details). In the early stages of the motion ($T < 0.4$ at $F_r = 0.38$) we again have good agreement with the Tyvand & Miloh method, in particular the numerical results support the prediction of asymmetry between free-surface deformations resulting from upwards and downwards cylinder motion, which arises in the analytical results because the second-order contribution η_2 acts upwards in either case, whereas the first-order contribution changes sign. This makes the trough in downwards motion less deep than the crest in the corresponding upwards motion. Again the numerical results can proceed in time significantly beyond the point when the analytical results become unreliable; for low-speed motion which does not result in breaking, the numerics may be continued indefinitely, allowing wave propagation outwards from the region near the cylinder.

For low-speed motion, however, a possible numerical problem is that of high-frequency waves being created from the impulsive cylinder motion; the situation is qualitatively similar to that of the impulsive pressure applied in the Cauchy–Poisson problem, see Lamb (1932). The slowly moving high-frequency waves are left behind the larger longer waves, and they appear to trigger numerical instabilities in our scheme if they are not smoothed. Nevertheless they have no practical effect on either the overall wave motion, nor on the hydrostatically dominated pressures on the already deeply submerged cylinder.

4. Free-surface deformations caused by submerging cylinders

We now look at the complete engulfment of the cylinder as it passes below the surface. The photographs of Greenhow & Lin (1983) are for the high-speed entry of a cylinder dropped from above the free surface; this causes rapidly moving spray jets which rise almost to the original drop height of the cylinder and then break up, presumably under the action of surface tension. Greenhow (1988) achieved partial success in following these jets, but could only follow the closure of the free surface over the top of the cylinder in a much less extreme case when the cylinder started from a half-submerged position in initially calm water. Inflow over the top of the cylinder caused the program to break down when the two layers of inrushing fluid (from left and right) impacted; see figure 4 for the present calculations. Although it is possible in principle to follow this symmetric situation further by placing a thin wall above the cylinder on the central plane of symmetry, so that the body + wall never actually submerges, no success was achieved. With hindsight numerical problems might have been expected since when a free-surface particle arrives at the intersection of the cylinder and wall, it will need to satisfy both the wall and cylinder body-boundary conditions, and thus be moving downwards initially, rather than rising up the wall as

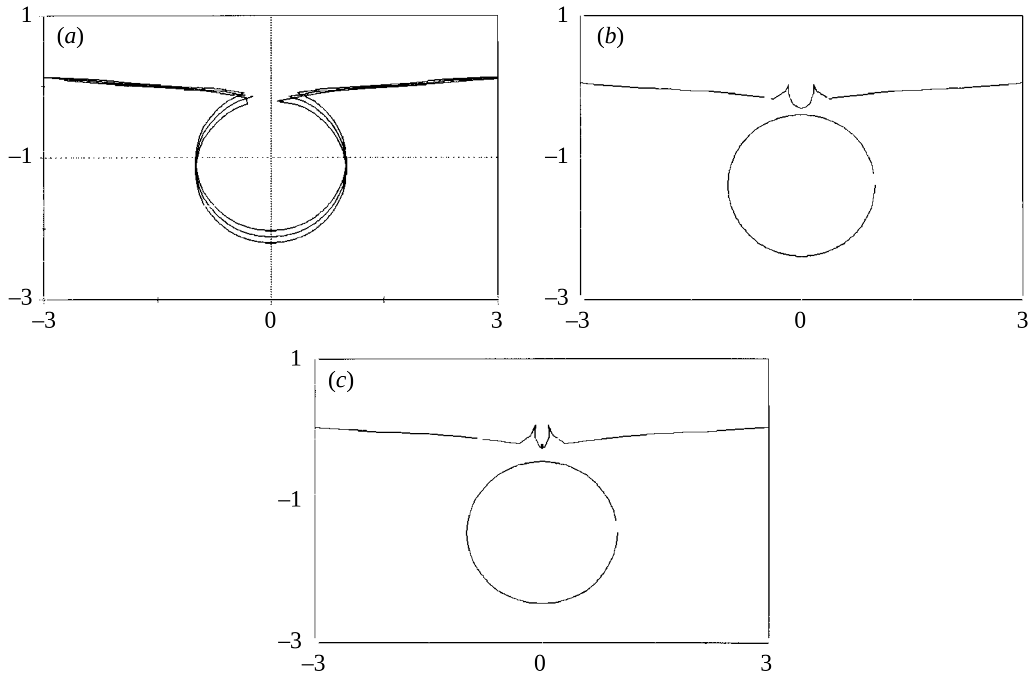

Figure 4. Vertical forced engulfment of a cylinder starting from rest half-submerged in initially calm water at Froude number = 0.31 for dimensionless times ($T = \sqrt{a/g}$); (*a*) $T = 1.82$, 1.96 and 2.1; (*b*) $T = 4.552$ showing the cavity and (*c*) $T = 4.75$ showing the start of jet formation.

a jet. Another problem is that this approach is not possible for oblique entry where no symmetry exists.

We here adopt a different approach to follow the flow, using the surface-piercing program initially and then swapping to the submerged program just as the body is totally engulfed when the simply connected fluid region becomes doubly connected. The situation is very similar to that of a collapsing bubble being threaded by a fast internal jet considered by Best (1993), see also Zhang *et al.* (1993). It should be noted that the values of ϕ on the left and right impacting free surfaces do not match immediately before impact for oblique entry, and its normal derivative does not match even for symmetric vertical entry (since the free surfaces are moving towards each other). Subject to some plausible assumptions concerning the integrability of the energy of the jet flow created immediately after impact, Best proves some important results, as follows.

(i) The free surface velocity potential away from the impacting surfaces is unaffected during the time of the impact; on the cylinder surface this may not be true in general, but we do not need to know the value of this jump *a priori* in the present numerical scheme.

(ii) The discontinuity across the impact surface of the tangential components of velocity before and after impact persists unaffected by the impact; in general this would create a vortex sheet and possible fluid rotation. In the present case, we assume the impact surface to lie approximately normal to the cylinder surface, being between the two inrushing very thin layers of fluid which are moving with the cylinder, so that their tangential velocity components along the impact surface will match.

(iii) The normal components of velocity across the impact surface, unequal before impact, must match afterwards.

(iv) Any discontinuity in velocity potential across the impact surface must persist, manifesting itself in circulation around the cylinder. In the present case, this will occur for oblique cylinder motion.

(v) The kinetic energy of the fluid will be conserved only in the case where the impact surface size shrinks to a point.

Point (iv) requires a branch cut in the analytic-function description of the flow. This is explicitly included in the submerged program, which can then continue calculations using the free-surface position and velocity potential as initial conditions. It is, of course, not possible to treat exactly the details of the impacting inrushing flows using the present approach; indeed compressibility effects may be needed. We assume impact occurs at a single point only, rather than across a surface, but the immediate resulting flow is unclear. Therefore a modification is needed to remove the two intersection points from the body by averaging over the positions and velocity potentials of the next nearest points. Other local collocation points were also added where needed (i.e. directly above the top of the cylinder since the inflow phase stretches out the surface points) by the same method; see Moyo (1997) for details. This has been shown to affect the flow only locally and only for a short time, so that the development of the subsequent flow is physically acceptable.

The forced motion of a cylinder, initially half-submerged in calm water, gives rise to extremely interesting free-surface deformations, see figure 4. A rapid inflow occurs over the cylinder top as it submerges. There is then a remarkably nearly constant hydrodynamic force acting upwards on the cylinder for a long period after the cylinder submerges. As mentioned above, the cylinder pressures, forces and dynamics are quite insensitive to the detailed motion of the free surface, especially the jets described below (except when the cylinder top is still very close to the free surface). Nevertheless it is still important to obtain accurate free surface calculations since fast moving jets appear, which, if not properly resolved, can lead to numerical breakdown. In the early stages after engulfment, the situation is qualitatively similar to the calculations of the collision of two solitary waves calculated by Cooker & Peregrine (1992). In their case the plane of symmetry represented a seawall, whereas in ours, the top of the cylinder might be thought of as giving the locally horizontal seabed, which, however, is moving downwards. Cooker & Peregrine's calculations also show cavity-like depressions at the seawall which rapidly 'flip through' to give a fast moving upwards jet of the type we see here in the last of figure 4. This phenomenon has also been photographed by Hattori *et al.* (1994). Following this jet requires very small time steps (at least an order of magnitude smaller than those used during the engulfment stage) and/or smoothing. We here adopt a procedure similar to that of Zhao & Faltinsen (1993) who remove spray jets occurring during wedge entry; details of when this is done may be found in Moyo (1997). It should be noted that the jets, being very thin, cannot support significant pressure gradients and their removal does not affect the surrounding fluid motion; although jet removal does slightly violate mass and energy conservation, the effect is also very small. The removal of the jet, whilst done primarily for numerical convenience, may also be necessary physically when the jet starts to fall; similar calculations with standing waves (see Srokosz 1981; Greenhow 1982), which support Penney & Price's (1952) conjecture that the sharpest stable standing-wave crest has an included angle of 90°, which is far larger than that of the thin jets created here. It follows that such jets will break-up during

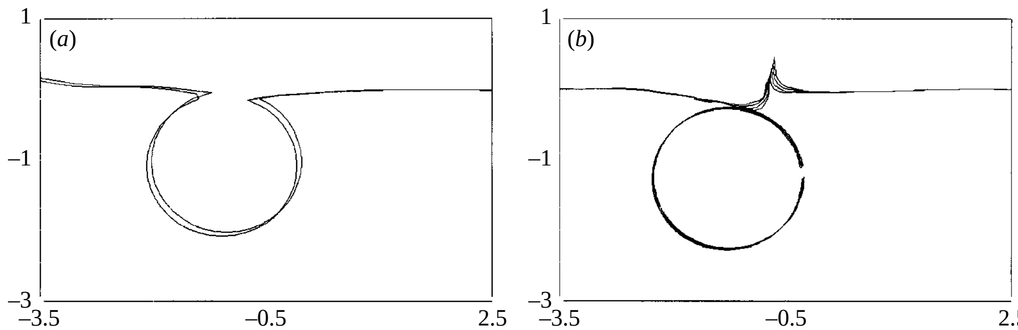

Figure 5. As for figure 4 but for 45° forced engulfment of a cylinder starting from rest half-submerged in initially calm water at a Froude number of 0.31 for (a) $T = 3.36$ and 3.558 and (b) $T = 5.80 \ldots 5.926$ in steps of 0.042.

their downwards motion, and this needs to be smoothed out or inhibited so that the calculations can continue to the wave propagation stage (not shown here). For certain free cylinder motion cases, the waves break symmetrically as two spilling breakers, and this finally stops the calculation. However, with less energetic fluid motion resulting from slower cylinder motion, non-breaking propagating waves may be possible so that the calculations could continue for much longer.

Figure 5 shows a case of forced entry at 45°. (For entry angles of 30° and 60°, at various Froude numbers, see Moyo (1997)). For low speed, the free surface stays fairly flat except for the very thin jet caused by the impacting fluid layers, associated with a high pressure region on the cylinder surface immediately below it. We do not claim that the calculation of the jet itself is accurate here; in reality the jet will quickly break up under the action of surface tension, but we again note that its details have no significance for the rest of the flow. Accordingly, for the medium speed calculations of figure 5, the jet is also removed, and the free surface is occasionally smoothed; see Moyo (1997) for figures and numerical details. This procedure allows the time-stepping to continue until the cylinder is rather deeply submerged, when the entire elevated region of the free surface starts to become unstable, causing numerical breakdown and global features such as the cylinder forces to become significantly affected. Accordingly we have not continued calculations beyond this time.

5. Conclusion

The calculations presented here for submerged cylinder forced motion show good agreement with the analytical time-expansion results of Tyvand & Miloh (1995a, b) for small time, after which interesting new features such as spontaneous breaking, high-frequency waves and outgoing breaking waves may arise. The situation, which contains three free parameters (depth-based Froude number, ratio of radius to initial depth of submergence and direction of motion) is complex, but we have covered enough of the parameter space to give an indication of how small time has to be for the expansion results to be valid. The study of downwards motion provided useful insights into results for the engulfment problem.

We also describe the forced engulfment of a vertically moving cylinder. The free surface displacement may be violent after the inrushing layers of water on top of the cylinder meet, creating a rapidly filling cavity and fast upwards moving jets. Oblique entry has also been considered.

PHILOSOPHICAL TRANSACTIONS OF THE ROYAL SOCIETY A MATHEMATICAL, PHYSICAL & ENGINEERING SCIENCES

S.M. thanks the Staff Development Committee of the National University of Science and Technology of Zimbabwe for financial support and leave of absence to undertake Ph.D. studies at Brunel University.

References

Barringer, I. 1996 *Water exit of two-dimensional bodies.* Loughborough: B.A.M.C.

Bassett, A. B. 1888 *A treatise on hydrodynamics.* Reprinted 1961. New York: Dover.

Best, J. P. 1993 The formation of toroidal bubbles upon the collapse of transient cavities. *J. Fluid Mech.* **251**, 79–107.

Brevig, P., Greenhow, M. & Vinje, T. 1981 Extreme wave forces on submerged cylinders. In *Proc. 2nd BHRA Int. Symp. on Wave and Tidal Energy*, Cambridge, pp. 143–166. British Hydraulics Research Association.

Cooker, M. J. & Peregrine, D. H. 1992 Wave impact pressure and its effect upon bodies lying on the sea bed. *Coastal Engng* **18**, 205–229.

Dean, W. R. 1948 On the reflection of surface waves from a submerged circular cylinder. *Proc. Camb. Phil. Soc.* **44**, 483–491.

Dold, J. W. & Peregrine, D. H. 1986 An efficient boundary-integral method for steep unsteady water waves. In *Numerical methods for fluid dynamics* (ed. K. W. Morton & M. J. Baines), vol. II, pp. 671–679. Oxford University Press.

Evans, D. V., Jeffrey, D. C., Salter, S. H. & Taylor, J. R. M. 1979 Submerged cylinder wave energy device: theory and experiment. *Appl. Ocean Res.* **1**, 3–12.

Garabedian, P. R. 1953 Oblique water entry of a wedge. *Commun. Pure Appl. Math.* **6**, 157–165.

Greenhow, M. 1982 Numerical simulation of standing waves in finite depth. *Adv. Water Resources* **5**, 185–189.

Greenhow, M. 1987 Wedge entry into initially calm water. *Appl. Ocean Res.* **9**, 214–223.

Greenhow, M. 1988 Water-entry and exit of a horizontal circular cylinder. *Appl. Ocean Res.* **10**, 191–198.

Greenhow, M. 1993 A complex variable method for the floating-body boundary-value problem. *J. Comput. Appl. Math.* **46**, 115–128.

Greenhow, M. & Li, Y. 1987 Added masses for circular cylinders near or penetrating fluid boundaries—review, extension and application to water-entry, exit and slamming. *Ocean Engng* **14**, 325–348.

Greenhow, M. & Lin, W.-M. 1983 Nonlinear free-surface effects: experiments and theory. Report, MIT, Department of Ocean Engineering, pp. 83–119.

Hattori, M., Arami, A. & Yui, T. 1994 Impact wave pressure on vertical walls under breaking waves of various types. *Coastal Engng* **22**, 79–114.

Haussling, H. J. & Coleman, R. M. 1979 Nonlinear water waves generated by an accelerating circular cylinder. *J. Fluid Mech.* **92**, 767–781.

Havelock, T. H. 1936 The forces on a circular cylinder submerged in a uniform stream. *Proc. R. Soc. Lond.* A **157**, 526–534.

Havelock, T. H. 1949*a* The wave resistance of a cylinder started from rest. *Q. Jl Mech. Appl. Math.* **2**, 325–334.

Havelock, T. H. 1949*b* The wave resistance of a submerged cylinder in accelerated motion. *Q. Jl Mech. Appl. Math.* **2**, 419–427.

Hepworth, T. 1991 An investigation of the motion of a submerged cylinder moving below a free surface with constant velocity. 4th year project report, Department of Mathematics and Statistics, Brunel University.

Howison, S. D., Ockendon, J. R. & Wilson, S. K. 1991 Incompressible water-entry problems at small deadrise angles. *J. Fluid Mech.* **222**, 215–230.

King, A. C. & Needham, D. J. 1994 The initial development of a jet caused by fluid, body and free-surface interaction. 1. A uniformly accelerating plate. *J. Fluid Mech.* **268**, 89–101.

Lamb, H. 1932 *Hydrodynamics*, VIth edn. Cambridge University Press.

Lin, W.-M., Newman, J. N. & Yue, D. K. P 1984 Nonlinear forced motions of floating bodies. In *15th Symp. Naval Hydrodynamics, Hamburg* (ed. W. C. Webster), pp. 33–49. Washington, DC: National Academy Press.

Longuet-Higgins, M. S. & Cokelet, E. D. 1976 The deformation of steep surface waves on water. I. A numerical method of computation. *Proc. R. Soc. Lond.* A **350**, 1–26.

Lui, Y. & Yue, D. K. P. 1996 On the time dependence of the wave resistance of a body accelerating from rest. *J. Fluid Mech.* **310**, 337–363.

Moyo, S. 1997 Hydrodynamic interaction of horizontal circular cylinders with a free surface. Ph.D. thesis, Brunel University. (In the press.)

Ogilvie, F. 1963 First- and second-order forces on a cylinder submerged under a free surface. *J. Fluid Mech.* **16**, 451–472.

Penney, W. G. & Price, A. T. 1952 Finite periodic stationary waves in a perfect liquid. *Proc. R. Soc. Lond.* A **244**, 254–284.

Roberts, A. J. 1987 Transient free-surface flows generated by a moving vertical plate. *Q. Jl Mech. Appl. Math.* **40**, 129–158.

Sakai, T., Husimi, Y. & Hatoyama, M. 1933 On the resistance experienced by a body moving in an incompressible perfect fluid towards its surface. *Proc. R. Soc. Japan* **15**, 4–11.

Srokosz, M. A. 1981 Breaking effects in standing and reflected waves. *Proc. Conf. Hydrodynamics in Ocean Engineering*, Trondheim, Norway.

Telste, J. G. 1987 Inviscid flow about a cylinder rising to a free surface. *J. Fluid Mech.* **182**, 149–168.

Terent'ev, A. G. 1991 Nonstationary motion of bodies in a fluid. *Proc. Steklov Inst. Math.* **186**, 211–221.

Tuck, E. O. 1965 The effect of non-linearity on flow past a submerged cylinder. *J. Fluid Mech.* **22**, 401–414.

Tyvand, P. A. & Miloh, T. 1995*a* Free-surface flow due to impulsive motion of a submerged circular cylinder. *J. Fluid Mech.* **286**, 67–101.

Tyvand, P. A. & Miloh, T. 1995*b* Free-surface flow generated by a small submerged circular cylinder starting from rest. *J. Fluid Mech.* **286**, 103–116.

Ursell, F. 1950 Surface waves on deep water in the presence of a submerged circular cylinder. *Proc. Camb. Phil. Soc.* **46**, 141–158.

Vinje, T. & Brevig, P. 1981*a* Nonlinear, two-dimensional ship motions. *Ship Res. Inst. Norway* R-112-81.

Vinje, T. & Brevig, P. 1981*b* Breaking waves on finite depth water; a numerical study. *Ship Res. Inst. Norway* R-118-81.

Vinje, T. 1989 On the small time expansion of nonlinear free surface problems. In *Proc. 4th Int. Workshop on Water Waves and Floating Bodies, Ostese, Norway* (ed. J. Grue), pp. 245–250.

Wagner, H. 1932 The phenomena of impact and planning on water. *NACA Translation* **1366**, 1–57.

Wu, G. X. 1993 Hydrodynamic forces on a submerged circular cylinder undergoing large-amplitude motion. *J. Fluid Mech.* **254**, 41–58.

Zhang, S., Duncan, J. H. & Chahine, G. L. 1993 The final stage of the collapse of a cavitation bubble near a rigid wall. *J. Fluid Mech.* **257**, 147–181.

Zhao, R. & Faltinsen, O. 1993 Water entry of two-dimensional bodies. *J. Fluid Mech.* **246**, 593–612.